Atmos. Meas. Tech. Discuss., 4, 4357–4401, 2011
www.atmos-meas-tech-discuss.net/4/4357/2011/
doi:10.5194/amtd-4-4357-2011

Atmospheric Measurement Techniques Discussions

Comparisons of temperature, pressure and humidity measurements by balloon-borne radiosondes and frost point hygrometers during MOHAVE 2009

D. F. Hurst[1,2], E. G. Hall[1,2], A. F. Jordan[1,2], L. M. Miloshevich[3], D. N. Whiteman[4], T. Leblanc[5], D. Walsh[5], H. Vömel[6], and S. J. Oltmans[2]

[1]Cooperative Institute for Research in Environmental Sciences, University of Colorado, Boulder, Colorado, USA
[2]NOAA Earth System Research Laboratory, Global Monitoring Division, Boulder, Colorado, USA
[3]Milo Scientific LLC, Lafayette, Colorado, USA
[4]NASA Goddard Space Flight Center, Greenbelt, Maryland, USA
[5]Jet Propulsion Laboratory, Table Mountain Facility, Wrightwood, California, USA
[6]Meteorologisches Observatorium Lindenberg, Deutscher Wetterdienst, Lindenberg, Germany

Received: 27 April 2011 – Accepted: 4 July 2011 – Published: 11 July 2011

Correspondence to: D. F. Hurst (dale.hurst@noaa.gov)

Published by Copernicus Publications on behalf of the European Geosciences Union.

Abstract

We compare coincident, balloon-borne, in situ measurements of temperature and pressure by two radiosondes (Vaisala RS92, Intermet iMet-1-RSB) and measurements of relative humidity (RH) by Vaisala RS92 sondes and frost point hygrometers. Data from a total of 28 balloon flights with mixed payloads are analyzed in 1-km altitude bins to quantify measurement biases between sensors and how they vary with altitude. The disparities between sensors determined here are compared to measurement uncertainties quoted by the two radiosonde manufacturers. Our comparisons expose several flight profiles with anomalously large measurement differences. Excluding these anomalous profiles, 33 % of RS92-iMet median temperature differences exceed the uncertainty limits calculated from manufacturer-quoted uncertainties. A statistically significant, altitude-independent bias of about $0.5 \pm 0.2\,^{\circ}\mathrm{C}$ is revealed for the RS92-iMet temperature differences. Similarly, 23 % of RS92-iMet median pressure differences exceed the quoted uncertainty limits, with 83 % of these excessive differences above 16 km altitude. The pressure differences are altitude dependent, increasing from -0.6 ± 0.9 hPa at the surface to 0.7 ± 0.1 hPa above 15 km. Temperature and pressure differences between redundant RS92 sondes on the same balloon exceed manufacturer-quoted reproducibility limits 20 % and 2 % of the time, respectively, with most of the excessive differences belonging to anomalous difference profiles. Relative humidity measurements by RS92 sondes are compared to other RS92 sondes and to RH values calculated using frost point hygrometer measurements and coincident radiosonde temperature measurements. For some flights the RH differences are anomalously large, but in general are within the ±5 % RH measurement uncertainty limits quoted for the RS92. The quantitative effects of RS92 and iMet pressure and temperature differences on frost point-based water vapor mixing ratios and RH values, respectively, are also presented.

AMTD

4, 4357–4401, 2011

1 Introduction

Vertical profile measurements of essential climate variables temperature, pressure and relative humidity have been made around the globe for decades. These measurements were predominantly made for weather forecasting and other short-term investigations, hence the collected data sets often lack the long-term stability and traceability necessary for climate research (Thorne et al., 2005; Titchner et al., 2009; Immler et al., 2010). Long-term measurement records from balloon-borne radiosondes are particularly questionable because of poorly documented instrument and procedural changes over the years (Titchner et al., 2009; Seidel et al., 2004).

This paper presents statistical evaluations of the differences between coincident, in situ, vertical profile measurements of temperature and pressure by two types of radiosondes; Vaisala RS92 and Intermet iMet-1-RSB. We also examine differences between relative humidity measurements by Vaisala RS92 radiosondes and two frost point hygrometers, the cryogenic frost point hygrometer (CFH; Vömel et al., 2007a) and the NOAA frost point hygrometer (FPH; Mastenbrook and Oltmans, 1983; Hurst et al., 2011). These balloon-borne measurements were made as part of the MOHAVE-2009 campaign, 11–27 October 2011 (Leblanc et al., 2011). We compare only measurements made from the same balloons, eliminating any concerns about spatial and temporal differences between the measurements by different sensors.

2 Experimental

A total of 44 balloons were launched during MOHAVE-2009 from the Table Mountain Facility (34.4° N, 117.7° W, 2285 m a.s.l.) near Wrightwood, California. Sixteen of these balloons carried a lone RS92 radiosonde. The remaining 28 balloons were instrumented with two or more radiosondes (Table 1). Twenty of these 28 balloons also carried an Intermet radiosonde and a frost point hygrometer; 16 with a CFH and 4 with

AMTD
4, 4357–4401, 2011

a NOAA FPH. Flights with two RS92 sondes on the same balloon made it necessary to designate one as primary and the other as secondary for the purpose of comparison.

All but two of the 28 balloon flights analyzed here were conducted at night to permit water vapor measurement comparisons between balloon-borne instruments and ground-based Raman lidars. Two balloons launched during daytime provided comparison data for FTIR spectroscopic measurements of water vapor (Table 1). Each balloon reached an altitude of at least 27 km except for four that burst prematurely.

2.1 Radiosondes

The Vaisala RS92 sondes used in this campaign were models SGP and K, the only difference being the GPS signal-receiving capability of the SGP. Both models include a capacitive wire temperature sensor, a pair of thin film capacitive polymer humidity sensors, a piezo-resistive silicon pressure sensor and a 403 MHz-band transmitter. Sensor data from each RS92 sonde were received and recorded every 2 s by a DigiCORA MW31 system. As specified by the manufacturer, RS92 humidity sensors removed from their packaging more than one hour before use were reconditioned within 30 min of launch by the Vaisala GC25 ground check system. Data transmission from the RS92 sondes ceased shortly after the start of descent therefore only ascent data were recorded.

Vaisala quotes two different types of measurement uncertainties pertinent to this comparison study: total measurement uncertainties in soundings, and measurement reproducibility for soundings with two sondes. Total quoted measurement uncertainty limits are <1 hPa (at >100 hPa) or <0.6 hPa (3–100 hPa) for pressure, <0.5°C for temperature, and <5 % RH for relative humidity. Measurement reproducibility limits are given as <0.5 hPa (>100 hPa) or <0.3 hPa (3–100 hPa) for pressure, <0.2° C (>100 hPa) or <0.3 °C (20–100 hPa) for temperature, and <2 % RH for relative humidity. It is noted here that all relative humidity values presented in this work are in units of % RH with respect to the saturation vapor pressure over liquid water (not ice), as these are the RH values reported by the DigiCORA MW31 system.

AMTD
4, 4357–4401, 2011

Relative humidity data from RS92 sondes were corrected based on a large body of research (Miloshevich et al., 2004, 2009; Vömel et al., 2007b). The corrections include adjustments for mean calibration bias, temperature-dependent sensor time-lag errors (only at $T < -45\,^{\circ}C$) and solar radiation errors (only for the two daytime flights). For the relatively dry tropospheric conditions observed during most MOHAVE 2009 balloon flights these corrections increased RS92 RH values by 1–3 % RH in the middle to upper troposphere. Note that Vaisala has recently implemented corrections in their DigiCORA software version 3.64 (December 2010) for 2 of the 3 measurement errors addressed in the MOHAVE 2009 RS92 data, namely time-lag errors and solar radiation errors.

The Intermet model iMet-1-RSB radiosondes used in this campaign include a bead thermistor temperature sensor, a piezo-resistive silicon pressure sensor, a capacitive polymer humidity sensor, a 12-channel GPS receiver, and a 403 MHz band data transmitter. In addition to transmitting their own sensor data, the iMet-1-RSB sondes also transmitted data from all connected CFHs, FPHs and ozonesondes. Sensor data from the iMet sondes and connected instruments were received by an Icom IC-R8500 receiver and recorded at non-uniform intervals of 1–3 s by custom software programs "STRATO" (iMet+CFH) and "SkySonde" (iMet+FPH). Data from iMet sondes were recorded during both the ascent and descent of balloons.

Intermet quotes pressure, temperature and relative humidity measurement uncertainties for its iMet-1-RSB radiosondes as accuracy limits of ±1.8 hPa (at >400 hPa) or ±0.5 hPa (4–400 hPa), ±0.3 °C, and ±5 % RH, respectively. Since there are no manufacturer-recommended or published corrections for the iMet-1-RSB measurements we compare the data as they were received and recorded.

2.2 Frost point hygrometers

The two frost point hygrometers flown during MOHAVE 2009 (CFH and FPH) utilize the same measurement principle and have many similar design features. Both instruments rely on the growth and maintenance of a stable frost layer on a temperature-controlled

AMTD
4, 4357–4401, 2011

mirror positioned within a steady air stream. A stable frost layer on the mirror implies equilibrium between the ice surface and the overlying air stream. At equilibrium the partial pressure of water vapor in the air stream is directly related to the mirror temperature (Brewer et al., 1948) through the Goff-Gratch formulation of the Clausius-Clapeyron equation (Goff, 1957). The frost point measurement technique relies on first principles and accurate calibrations of thermistors embedded in the mirrors; no water vapor calibration standards or scales are required.

Both frost point hygrometers stem from the fundamental design and operational principles of the NOAA FPH that was first flown over Boulder, Colorado in 1980 (Mastenbrook and Oltmans, 1983). CFH technology diverged from the FPH in 2003 through efforts to reduce instrument size and weight, improve frost layer stability and eliminate the need for a sun shield (Vömel et al., 2007a). Both instruments have been significantly improved throughout the years, but since these improvements were not exactly the same for the CFH and FPH, the two instruments diverged in subtle ways. Stratospheric water vapor mixing ratios calculated from CFH and FPH launched together on 5 different balloons from Boulder, CO, during 2008–2009 differed by an average 0.1 ± 0.2 ppmv, about 2 % of the stratospheric water vapor mixing ratio (Hurst et al., 2011).

2.3 Data matching

There were no simultaneous releases of multiple balloons during this campaign (Table 1) so every comparison performed here is strictly between instruments on the same balloon. We find it most reliable to match data from the instruments on the same balloon by their time stamps, largely because matching methods based on sensor data can potentially be skewed by sensor biases. Timestamp matching is free from such biases because each sounding system reliably records measurement timestamps as elapsed time since launch. A sounding system is defined here as each of the three unique combinations of radiosondes and software programs mentioned in Sect. 2.1. Timestamp matching can be tricky, however, because the three sounding systems use

AMTD
4, 4357–4401, 2011

slightly different algorithms to detect the moment of balloon launch based on their own radiosonde's sensor data. This makes it imperative that the elapsed timestamps of the different sounding systems are adjusted to a common time of launch for each flight before the in-flight data are compared.

Timestamp adjustments between the different sounding systems were determined for each balloon flight using two methods. The first was to shift timestamps of the primary RS92 relative to those of the other radiosonde(s) on each balloon, incrementally in 2 s intervals, to find the timestamp adjustment that maximizes the correlation coefficient (r) between coincident temperature measurements. The maxima in correlation coefficients were clearly defined for 85 % of these temperature data comparisons. The second method was to visually inspect the two time series of coincident temperature measurements, looking for temporal offsets in observed temperature features. Temperature data were used in both approaches because, unlike the relatively smooth decrease of pressure with altitude, there are often significant deviations (features) of temperature from the standard lapse rate. The second method provided good corroboration of the first method and suggested realistic timestamp adjustments for the remaining 15 % of flights.

Timestamp adjustments for the 20 primary and 6 secondary RS92 sondes relative to timestamps of the 20 iMet sondes (Table 1) averaged 2.5 ± 6.0 s with minimum and maximum adjustments of -12 s and 16 s, respectively. For the 8 flights with only dual RS92 sonde payloads, adjustments to primary RS92 timestamps relative to secondary RS92 timestamps were smaller, with an average of 0.0 ± 2.5 s, minimum of -8 s, and maximum of 2 s. In most cases these timestamp adjustments significantly improved agreement between the sensor data from the different radiosondes, not only for temperature but also for pressure and relative humidity.

After the timestamps were matched, data from the 26 RS92 sondes on balloons with iMet sondes were interpolated to the timestamps of the iMet data. Gaps > 6 s in RS92 data were not interpolated. Comparisons between data from primary and secondary RS92 sondes did not require interpolation because timestamp shifts (if any) were in

AMTD
4, 4357–4401, 2011

multiples of 2 s, the exact intervals at which RS92 data were recorded. We reiterate here that since RS92 sonde data are for balloon ascent only the following comparisons include no descent data.

3 Comparisons

Measurement differences are calculated from the time-matched data of two sensors on the same balloon. Differences between redundant RS92 sondes on the same balloon were always calculated by subtracting secondary sonde data from primary sonde data. For comparisons between RS92 sonde data and either iMet sonde or frost point hygrometer data we consistently subtract the latter from the former. Median measurement differences are determined in 1-km altitude bins to create an altitude profile of differences for each comparison. We employ median instead of average differences to reduce the influences of any large, random measurement differences on our investigation of measurement biases. The median differences for all profiles, and for a subset "majority of profiles" that excludes any anomalous profiles, are compared to manufacturer-quoted measurement uncertainties and statistically examined for biases. We also compute statistics for the measurement differences in each of six 5-km altitude bins (0–30 km) to check for altitude-dependent measurement biases.

3.1 Temperature

Vertical profiles of differences between coincident temperature measurements by RS92 and iMet sondes expose some significant biases as well as random disparities caused by sporadic sensor noise (Fig. 1). Eight of these 26 difference profiles stand out from the majority of profiles. These anomalous profiles are plotted using colored markers and identified in figure legends by their profile number. Profile numbers comprised of the flight number and suffix "*b*" denote comparisons between secondary RS92 sondes and iMet sondes. From here forward we use the label "anomalous" to describe

AMTD
4, 4357–4401, 2011

difference profiles that do not conform to the majority of profiles. Difference profiles repeatedly identified as anomalous are plotted using markers of a consistent color throughout this work. Black markers always represent the majority of profiles in the difference profile plots.

To focus more on measurement biases and less on noise it is preferable to plot each of the RS92-iMet temperature difference profiles as median differences in 1-km altitude bins (Fig. 2). Note that the same 8 anomalous difference profiles identified in Fig. 1 also stand out from the majority of profiles in Fig. 2. In many cases our use of median difference values reduces noise and allows the difference profiles to be plotted together using smaller x-axis ranges that increase clarity. Vertical profiles of 1-km median temperature differences between redundant RS92 sondes on the same balloon (Fig. 3) also expose several anomalous difference profiles around a well-defined majority of profiles. Five non-conforming RS92-RS92 temperature difference profiles are identified. Anomalous profiles of measurement differences between redundant RS92 radiosondes on the same balloon are identified by flight number.

We examine the 1-km median temperature differences against manufacturer-quoted measurement uncertainty values that were presented in Sect. 2.1. For RS92-iMet differences the RS92 total uncertainties and iMet accuracy values are combined in quadrature to arrive at uncertainty limits of ±0.58 °C. For RS92-RS92 differences the manufacturer's measurement reproducibility values are quoted for two different pressure regimes. To complement our scheme of binning measurement differences by altitude, we transform the manufacturer-quoted pressure boundaries of 400 and 100 hPa into altitude boundaries of 7 and 16 km, respectively. The altitude-bounded temperature measurement reproducibility limits for redundant RS92 sondes are combined, in quadrature, yielding uncertainty limits of ±0.28 °C (<16 km) and ±0.42 °C (>16 km).

RS92-iMet 1-km median temperature differences in all 26 profiles (Fig. 2) exceed the combined manufacturer-quoted uncertainty limits 39 % of the time. This fraction drops to 33 % if the 8 anomalous difference profiles are excluded. Two-thirds of the excessive RS92-iMet temperature differences in the 18 non-anomalous profiles are in

AMTD
4, 4357–4401, 2011

the 14–22 km altitude range (Fig. 2) and nearly 70 % of all differences in this layer exceed the uncertainty limits. Curiously, every 1-km median temperature difference in the two anomalous profiles TF028 and TF028b is within ±0.3 °C (Fig. 2), well inside the ±0.58 °C uncertainty limits.

Median RS92-RS92 temperature differences in all 14 profiles (Fig. 3) exceed the combined reproducibility limits 20 % of the time. All but two of the excessive differences belong to one of the five anomalous difference profiles. Only 1 % of temperature differences in the majority of profiles (Fig. 3) exceed the combined uncertainty limits.

Attribution of an anomalous difference profile to irregular data from a specific radiosonde is possible for any of the 6 flights with one iMet and two RS92 sondes through visual comparison of the three difference profiles. For example, RS92-RS92 temperature differences for flight TF028 are small (Fig. 3) while the two RS92-iMet difference profiles TF028 and TF028b are similarly anomalous (Fig. 2). The two anomalous difference profiles for this flight are therefore likely caused by irregular iMet temperature data. Similarly, temperature data for the secondary RS92 sonde TF025b are deemed irregular because RS92-iMet differences (TF025) are small (Fig. 2) while the RS92-RS92 TF025 (Fig. 3) and RS92-iMet TF025b (Fig. 2) difference profiles are both anomalous and roughly mirror images.

The 1-km median differences in each set of temperature comparison profiles are sorted into cumulative distribution functions (CDFs, Fig. 4). The CDFs display the fractions of median differences in all profiles (dashed curves), or in the majority of profiles (solid curves), that are less than the specified temperature differences (bottom axis). In general, CDFs computed from all difference profiles (Fig. 4, dashed curves) are skewed from normal by large differences in the anomalous profiles, while those determined from only non-anomalous profiles (Fig. 4, solid curves) are more normally distributed. In some cases even near-normal CDFs are shifted positively or negatively from zero, reflecting potential biases between sensors.

To test the statistical significance of biases between sensors we calculate the mean, median, standard deviation range (mean $-1\,\sigma$ to mean $+1\,\sigma$) and inner-68 % range

AMTD
4, 4357–4401, 2011

(16th to 84th percentiles depicting the standard deviation range of a normal distribution) of differences (Table 2). The inner-68 % ranges can be read from the CDFs while the standard deviation ranges are displayed separately as horizontal error bars to the right of the CDFs (Fig. 4). There is good agreement between the mean and median, and between the standard deviation and inner-68 % ranges of each set of temperature differences in the majority of profiles (Table 2). This agreement implies that the information garnered from CDFs and Gaussian statistics can be meshed together in a meaningful way, but in no way does it definitively indicate that the temperature differences are normally distributed. Combining information from the CDFs and Gaussian statistics, we consider a bias statistically significant if both the standard deviation range and the inner-68 % range do not cross zero, as is the case for the majority of profile differences between RS92 and iMet temperatures (Table 2, Fig. 4). If one range crosses zero but the other does not the significance of the bias is deemed marginal.

The CDF for all 14 RS92-RS92 temperature differences (Fig. 4) depicts a median of −0.02 °C and inner-68 % range of −0.43 to 0.13 °C compared to a mean of −0.15 °C and standard deviation range of −0.63 to 0.33 °C (Table 2). These statistics and the CDF suggest that the distribution of all RS92-RS92 temperature differences is negatively skewed (Fig. 4) by the large negative differences in the two highly anomalous profiles (Fig. 3). RS92-RS92 differences in the 9 non-anomalous profiles have a mean (0.04 °C) and standard deviation range (−0.06 to 0.14 °C) much more in line with the median (0.05 °C) and inner-68 % range (−0.04 to 0.13 °C), implying a more normal distribution of the differences. These statistics expose no significant bias between temperature measurements by redundant RS92 sondes on the same balloons for the non-anomalous profiles.

A similar evaluation of the RS92-iMet temperature differences is performed. The CDFs for all 26 RS92-iMet difference profiles and for the 18 non-anomalous difference profiles appear fairly normal (Fig. 4) though the former CDF is somewhat spread by the many large anomalous profile differences. For the 18 non-anomalous profiles the mean (0.50 °C) and standard deviation range of (0.26 to 0.74 °C) compare well with

AMTD
4, 4357–4401, 2011

the median (0.49 °C) and inner-68 % range (0.29 to 0.70 °C). Both CDFs for RS92-iMet temperature differences are positively shifted from zero by about 0.5 °C (Fig. 4), suggesting a potential bias. Neither the standard deviation nor inner-68 % range crosses zero, therefore the mean and median differences (0.50 and 0.49 °C) represent a significant bias.

The CDFs and Gaussian statistics for profile differences can expose significant biases between two sensors, but a lack of overall bias doesn't preclude significant biases that might vary with altitude. No significant bias was found for the RS92-RS92 temperature differences (Fig. 4, Table 2), but this could be the fortuitous result of negative biases at low altitudes cancelling out positive biases at high altitudes (or vice-versa). Interestingly, some of the anomalous RS92-iMet temperature difference profiles (Fig. 2) have small and conforming values at the surface that grow to larger, anomalous values at higher altitudes. Other anomalous profiles (Fig. 2) have large differences at the surface that decrease with altitude but never conform to the non-anomalous profiles. In contrast, all of the anomalous RS92-RS92 temperature difference profiles have non-conforming differences all the way from the surface to the highest altitudes (Fig. 3). The root cause(s) of these and other anomalous difference profiles remain(s) unclear but may include sensor production variability including calibration, sensor damage before launch, or sensor measurements being compromised by RF interference from radiosonde transmitters.

To further explore temperature measurement differences and their behavior with altitude we binned the 1-km median differences for all non-anomalous profiles into 5-km altitude layers and computed CDFs and Gaussian statistics for each bin. A layer width of 5 km was chosen to populate each bin with an adequate number of 1-km median differences and to simplify the plots and interpretation of the altitude-dependent statistics. As with the CDFs and Gaussian statistics for all temperature differences, agreement between the mean and median, and between the standard deviation and inner-68 % ranges in each 5-km altitude bin are considered indicators of near-normal difference distributions. For the RS92-iMet temperature differences, statistically significant biases

AMTD
4, 4357–4401, 2011

are exposed in every 5-km bin, with mean and median values varying from 0.3 to 0.7 °C. Here again we link bias significance to the fact that both the standard deviation and inner-68 % ranges do not cross zero (Fig. 5). Though there is some visual hint of altitude dependence in the RS92-iMet biases, overlap between the wide standard deviation and inner-68 % ranges in the 6 altitude bins precludes a statistically significant altitude dependence. The same statistical analysis of RS92-RS92 differences in 5-km altitude bins reveals no significant biases in the 6 altitude layers (Fig. 5).

3.2 Pressure

Five of the 26 RS92-iMet pressure difference profiles stand out as anomalous relative to the majority of profiles (Fig. 6). Just over 30 % of the pressure differences in all 26 RS92-iMet profiles exceed the combined uncertainty limits of ±2.06 hPa (<7 km), ±1.12 hPa (7–16 km) or ±0.78 hPa (>16 km). Exclusion of the 5 anomalous differences profiles lowers the fraction of excessive differences to 23 %. The vast majority (83 %) of excessive differences are above 16 km altitude (Fig. 6) where the quoted uncertainty limits are smallest. A close visual inspection of the majority of difference profiles (Fig. 6) suggests there may be a negative bias at the surface and a positive bias at high altitudes.

Pressure differences for the 14 dual-RS92 profiles are smaller and more consistent (Fig. 7) than the RS92-iMet pressure differences (Fig. 6). None of the profiles are considered anomalous and only 2 % of all RS92-RS92 pressure differences exceed the combined reproducibility limits of ±0.71 hPa (<16 km) or ±0.42 hPa (>16 km). All 7 excessive pressure differences are below 5 km. There is some visual indication of a small negative bias in the 14 RS92-RS92 pressure difference profiles.

As for temperature, it is possible to identify the radiosonde with anomalous pressure data for the flights with 3 radiosondes. There is only one such flight (TF025) with anomalous profiles (TF025 and TF025b) of RS92-iMet pressure differences (Fig. 6). The similarity of these two anomalous difference profiles (Fig. 6) and the small differences between the primary and secondary RS92 sondes (Fig. 7) suggest that the iMet

AMTD
4, 4357–4401, 2011

pressure data for this flight are irregular. Four of the five anomalous RS92-iMet profiles have large differences at the surface but above 20 km the differences in all five anomalous profiles conform to the majority of profiles.

For RS92-iMet pressure differences in the majority of profiles there is good agreement between the mean (0.35 °C) and median (0.43 °C), and between the standard deviation range (−0.33 to 1.03 hPa) and inner-68 % range (−0.29 to 1.00 hPa), respectively. CDFs for the RS92-iMet pressure differences illustrate how large negative pressure differences in the anomalous profiles (Fig. 6) skew the CDF for all profile differences (Fig. 8). The two RS92-iMet CDFs agree above the 50th percentile, are both positively shifted from zero, and have 60th and 84th percentiles that indicate a positive bias of 0.5–1.0 hPa (Fig. 8). However, even with the mean and median differences also suggesting a 0.4 hPa bias, the variability of differences in the non-anomalous profiles is large enough to spread both the inner-68 % and standard deviation ranges across zero (Table 2).

The CDFs and Gaussian statistics of RS92-RS92 pressure differences in all 14 profiles (Fig. 8, Table 2) indicate they are normally distributed with a mean and median of −0.14 hPa. The two CDFs are exactly the same because none of the difference profiles are anomalous. The inner-68 % and standard deviation ranges agree well (−0.35 to 0.04 and −0.37 to 0.09 hPa, respectively) and neither exposes a significant bias. The inner-90 % range (5th to 95th percentile) of RS92-RS92 pressure differences in all 14 profiles spans only −0.55 to 0.14 hPa (Fig. 8) because there are no anomalous difference profiles.

The importance of altitude-dependent difference statistics is clearly demonstrated by the vertical profiles of the RS92-iMet pressure differences (Fig. 9). Overall statistics for these differences expose no significant bias (Table 2), but the 5-km altitude-binned statistics certainly do (Fig. 9). Mean and median differences in the 5-km altitude bins increase with altitude from −0.6 hPa (0–5 km) to 0.8 hPa (25–30 km), but only above 15 km are these biases statistically significant (Fig. 9). Agreement between the mean and median, and between the inner-68 % and standard deviation ranges in each bin attests

AMTD
4, 4357–4401, 2011

to near-normal distributions of the binned differences. Without several large pressure differences near the surface that deny statistical significance to the negative bias in the 0–5 km bin there would be a smooth transition of the pressure biases from about −0.6 hPa at the surface to 0.6–0.8 hPa above 15 km. None of the 5-km binned RS92-RS92 pressure biases are significant although the standard deviation ranges above 20 km do not cross zero, exposing marginally significant −0.1 hPa biases.

3.3 Relative humidity

Three of the 14 vertical profiles of relative humidity (RH) differences between redundant RS92 sondes are anomalous (Fig. 10). There is little indication from the surface RH data that the measurements by these 3 sondes would be problematic at higher altitudes. Only 4 % of the 1-km median differences in all 14 profiles exceed the combined reproducibility limits of ±2.8 % RH, and each belongs to one of the three anomalous profiles (Fig. 10). We note that RH differences above 20 km altitude are unlikely to exceed the combined reproducibility limits (±2.8 % RH) because 95 % of the RH values measured at these altitudes are <3 % RH (Fig. 10). However, since there appears to be no altitude dependence whatsoever for the RS92-RS92 RH differences (Fig. 10) we include RH differences above 20 km in the statistical analysis. This will not be the case for the other RH measurement comparisons that show large drops in the differences above 20 km.

Comparisons between RS92 and iMet relative humidity measurements are not presented here because the iMet humidity sensors were problematic during the campaign. Measurement glitches, especially data dropouts with negative RH values, posed the greatest difficulty. Since October 2009, Intermet has worked to re-implement the capacitive polymer humidity sensor in their iMet-1-RSB radiosondes. Some of our more recent balloon flights with these radiosondes suggest that the data dropouts have been eliminated.

Instead we examine differences between frost point hygrometer-based RH values calculated using RS92 temperatures (FP_{RS92}) and using iMet temperatures (FP_{IMET}).

AMTD
4, 4357–4401, 2011

The calculation of RH from frost point hygrometer measurements of the partial pressure of water vapor (Pw) requires coincident measurements of air temperature by the accompanying radiosonde(s). Temperature determines the saturation vapor pressure over liquid water (Psat) that is needed to convert Pw to % RH (= 100*Pw/Psat). We note again here that the RS92 RH values compared in this work have been corrected using well-documented algorithms. The impacts of these corrections for the MOHAVE 2009 campaign are illustrated in Fig. 1 of Leblanc et al. (2011).

Differences between frost point hygrometer-based % RH values calculated using RS92 temperatures (FP_{RS92}) and iMet temperatures (FP_{IMET}) are displayed as vertical profiles of 1-km bin medians (Fig. 11). Seven of the 26 difference profiles are considered anomalous. The only sources of RH disparities here are RS92-iMet temperature differences so it is not surprising that 4 of the 7 anomalous RH difference profiles (Fig. 11) were also deemed anomalous for temperature differences (Fig. 2). However, the relationship between temperature differences and RH differences is not simple because of the non-linear nature of the Clausius-Clapeyron equation that determines Psat. The dependence of RH on temperature is inverse, meaning a positive temperature bias (Fig. 2) will produce a negative RH bias (Fig. 11), but the same temperature bias at high and low temperatures will have very different effects on the % RH value.

Since we present RH differences in absolute units the % RH differences induced by temperature differences are solely a function of temperature unless the RH value is small enough to limit the % RH differences. A big temperature difference at low temperature may not result in as large a difference in % RH as a smaller temperature difference at high temperature. This helps explain why the 2–3 °C temperature differences at 4–7 km in profile TF025b (Fig. 2) induce only 1.5 % RH differences (Fig. 11) while <1 °C temperature differences at 10–12 km in profile TF041b (Fig. 2) lead to differences > 6 % RH. As mentioned above, low RH values above 20 km (Fig. 11) preclude FP_{RS92}-FP_{IMET} RH differences from exceeding 3 % RH so the FP_{RS92}-FP_{IMET} RH differences above 20 km are omitted from the analysis.

AMTD
4, 4357–4401, 2011

Figure 12 presents the CDFs of RH differences between redundant RS92 sondes and between frost point hygrometer-based RH values (FP_{RS92}-FP_{IMET}). Only for the RS92-RS92 comparisons are the RH differences above 20 km included. Each of these CDFs is negatively skewed and negatively shifted from zero, but both the skew and shift are reduced in magnitude through exclusion of large negative differences in the anomalous profiles. The CDF, mean, and median for the majority of RS92-RS92 RH difference profiles together suggest a bias of −0.3 % RH (Table 2, Fig. 12), but neither the standard deviation range nor inner-68 % range (both −0.7 to 0.1 % RH) support this (Table 2). The mean, median and CDF for the majority of FP_{RS92}-FP_{IMET} difference profiles together suggest a bias of -0.5 ± 0.1 % RH below 20 km (Table 2, Fig. 12), a sensible suggestion given the positive RS92-iMet temperature biases at these altitudes (Fig. 5). The standard deviation range of FP_{RS92}-FP_{IMET} RH differences (−1.3 to 0.1 % RH) crosses zero but the inner-68 % range does not (−1.0 to −0.1 % RH), indicating a bias with marginal statistical significance.

None of the 5-km bin means and medians of RH differences for redundant RS92 sondes are statistically significant, but the inner-68 % range (−0.56 to −0.06 % RH) of the 0–5 km bin and standard deviation range (−0.56 to −0.02 % RH) of the 25–30 km bin suggest marginally significant negative biases (Fig. 13). Mean and median FP_{RS92}-FP_{IMET} RH differences are negative and statistically different from zero in the 10–15 and 15–20 km bins (Fig. 13) while the 0–5 and 5–10 km bins reveal only marginal negative biases. This is somewhat surprising given that RS92-iMet temperature biases were significantly positive in every 5-km altitude bin (Fig. 5). Our method of assessing biases using both CDFs and Gaussian statistics seems to yield more cases of marginal biases for RH measurements, likely because the distributions of RH measurement differences are less normal than those of pressure and temperature differences.

Armed with a better understanding of the magnitudes of frost point-based RH differences induced by RS92-iMet temperature differences we now compare frost point-based RH values with direct RH measurements by the RS92 sondes. Interestingly, even the largest RH differences induced by radiosonde temperature differences

AMTD
4, 4357–4401, 2011

(Fig. 11) are dwarfed by the 10–25 % RH disparities between the RS92 and frost point-based measurements (Figs. 14 and 15). Except for TF042 the four anomalous profiles are similar in both Figs. 14 and 15, indicating that RS92-iMet temperature differences contribute little to these much larger RH measurement differences. Based solely on the quoted ±5 % accuracy limits for RS92 RH measurements about 9 % of RS92-FP_{RS92} and 10 % of RS92-FP_{IMET} RH differences are excessive. These are predominantly associated with the anomalous difference profiles (Figs. 14 and 15).

A quick comparison of anomalous difference profiles can help identify the instrument that produced irregular RH data for two flights. For flight TF025 there are large RH differences between the primary and secondary RS92 sondes (Fig. 10) and between the secondary RS92 sonde and the CFH (TF025b, Figs. 14 and 15), but not between the primary RS92 sonde and the CFH (TF025, Figs. 14 and 15). This evidence points to high-biased RH measurements by the secondary RS92 sonde (TF025b) in the 10–13 km layer. For flight TF041 the similar and large RH differences between both RS92 radiosondes and the CFH (TF041 and TF041b, Figs. 14 and 15) and the good agreement between the two RS92 sondes (TF041, Fig. 10) suggest a high bias in the CFH-based RH values between 5 and 12 km. The source of irregular RH data for TF026 (Figs. 14 and 15) cannot be identified because only one RS92 sonde was flown.

The majority of difference profiles in each of the RS92-frost point RH comparisons visually hint at negative biases (Figs. 14 and 15). The CDFs of all 26 profiles of RS92-FP_{RS92} and RS92-FP_{IMET} RH differences are negatively skewed and shifted by the large negative differences in anomalous profiles TF041 and TF042. Excluding the anomalous profiles makes the distributions of differences more normal, but the CDFs for the majority of differences remain negatively shifted from zero (Fig. 12), suggesting potential biases. The standard deviation and inner-68 % ranges of RS92-FP_{RS92} RH differences expose no significant negative bias (Table 2) even though the CDF for the majority of profiles does not cross zero until the 80th percentile. The inner-68 % range of RS92-FP_{IMET} RH differences exposes a marginal bias of about −1.2 % RH without corroboration by the standard deviation range (Fig. 12, Table 2).

AMTD
4, 4357–4401, 2011

The altitude-dependent statistics (Fig. 16) reveal significant negative biases in RS92-FP_{IMET} differences between 10 and 20 km, a significant negative RS92-FP_{RS92} bias (15–20 km), a marginally significant negative RS92-FP_{IMET} bias (0–5 km) and a marginally significant negative RS92-FP_{RS92} bias (10–15 km). None of these biases are larger in magnitude than −2 % RH, well within the RS92 RH measurement uncertainties. Statistically significant biases of 0.6 ± 0.3% RH are exposed in both sets of differences at 25–30 km, but according to Miloshevich et al. (2009) the RH correction algorithms are not truly appropriate for the very low RH conditions observed above ∼20 km during MOHAVE 2009.

3.4 Water vapor mixing ratios

Here we compare water vapor volume mixing ratios calculated from the frost point hygrometer measurements (Pw) using coincident pressure measurements by the RS92 and iMet sondes. Given that water vapor mixing ratios at the surface can be 10 000 times stratospheric values of 3–5 ppmv, we present statistics for water vapor mixing ratio differences relative to the mixing ratios themselves, in percentage units. Statistics for all 26 RS92-iMet difference profiles (FP_{RS92}-FP_{IMET}) reveal no significant bias in the relative mixing ratio differences (Table 2). The mean (−0.5 %), median (0.0 %), standard deviation range (−2.2 to 1.1 %) and inner-68 % range (−1.7 to 0.2 %) together indicate a negative skew in the distribution of differences.

Simplistically, volume mixing ratios are inversely proportional to the atmospheric pressure such that a positive pressure bias induces a negative mixing ratio bias. Since the only sources of mixing ratio differences here are pressure differences between the RS92 and iMet sondes, the vertical profiles of 1-km median relative mixing ratio differences (not shown) look very much like mirror images of the RS92-iMet pressure difference profiles (Fig. 6).

Altitude-dependent statistics for the relative mixing ratio differences (FP_{RS92}-FP_{IMET}) in 5-km altitude bins reveal significant negative biases (−2 to −4 %) above 20 km (Fig. 17). Vertical profiles of RS92-iMet pressure differences (Fig. 9) and relative mixing

AMTD
4, 4357–4401, 2011

ratio differences (Fig. 17) are not perfect mirror images; the altitude-dependent decrease in relative mixing ratio biases above 15 km is more dramatic than the increase in pressure biases. This stems from small pressure differences (0.5–0.8 hPa) becoming large relative pressure differences (2–4 %) as atmospheric pressure drops to near 20 hPa. The mixing ratio biases above 20 km (Fig. 17) approach the relative uncertainties of stratospheric water vapor measurements by the CFH and FPH, illustrating the need for high accuracy radiosonde pressure measurements to convert frost point hygrometer measurements into accurate water vapor mixing ratios.

3.5 Altitude

Here we compare in-flight altitudes calculated by the Vaisala DigiCORA software using RS92 measurements and those computed by both the STRATO and SkySonde programs using iMet measurements. In-flight altitude changes are calculated incrementally by each sounding system using the hypsometric equation. The equation relates changes in air density, calculated from measured increments in pressure, temperature and RH as the balloon rises or falls, to changes in altitude. Pressure, temperature and RH measurements at the known altitude of the launch site provide the initial basis for these calculations. Incremental changes in altitude are cumulatively summed to provide an estimate of the balloon altitude at each timestamp after launch.

Biased measurements of pressure, temperature or RH may or may not induce biases in the calculated altitudes because altitude changes are computed from small measured differences in these variables. Differences computed from sequential measurements afflicted by a constant offset (i.e. bias with no altitude dependence) are exactly the same as the differences computed from unbiased measurements. In contrast, a measurement bias that changes with altitude will induce an altitude-dependent bias in sequential measurement differences and therefore a bias in the computed altitude increments. Altitudes calculated in this way are susceptible to altitude-dependent biases because the cumulative effects of even small biases in measurement differences can become large.

AMTD
4, 4357–4401, 2011

Statistics for the altitude differences between primary and secondary RS92 sondes and between the RS92 and iMet sondes (Table 2) expose no significant biases. Most of the differences between redundant RS92 sondes are quite small; the standard deviation and inner-86 % ranges are −0.04 to 0.04 and 0.01 to 0.02 km, respectively. For RS92-iMet differences these ranges are −0.15 to 0.07 and −0.13 to 0.04 km, respectively.

Altitude-dependent statistics in 5-km bins for both sets of altitude differences are shown in Fig. 18. The RS92-RS92 differences show no significant biases (Fig. 18) while the RS92-iMet differences are significantly biased only above 25 km. This significant bias above 25 km is presumably caused by the altitude-dependent RS92-iMet pressure differences (Fig. 9). We must also consider the possibility that the hypsometric algorithms in the Vaisala DigiCORA software may be slightly different from those in the STRATO and SkySonde programs. Overall, the altitudes calculated by the different sounding systems using input from their specific radiosondes agree to better than 0.1 km below 20 km, 0.2 km between 20 and 25 km, and 0.4 km in the 25–30 km layer.

4 Summary

We have rigorously compared coincident in situ measurements of temperature and pressure by RS92 and iMet-1-RSB radiosondes on the same balloons, along with RH measurements by RS92 sondes and frost point hygrometers. Profiles of median differences in 1-km altitude bins were constructed for each sensor pair, and for every comparison (except RS92-RS92 pressure differences) several profiles were identified as non-conforming to the majority of profiles (anomalous). The anomalous profiles did not consistently link to poor measurement agreement between sensors at the surface.

Profile differences were examined against uncertainty limits determined from manufacturer-quoted measurement uncertainty and reproducibility limits. The fractions of 1-km median differences found to exceed these uncertainty limits were: RS92-RS92 temperature (20 %), RS92-iMet temperature (39 %), RS92-RS92 pressure (2 %),

AMTD
4, 4357–4401, 2011

RS92-iMet pressure (30 %), RS92-RS92 relative humidity (4 %), and RS92-frost point hygrometer relative humidity (10 %).

Profile differences were analyzed for biases using cumulative distribution functions (CDFs) and Gaussian statistics. Only non-anomalous profiles were considered in these analyses to gauge the magnitudes of "typical" biases (i.e. without the artifacts of anomalous profiles). Biases were deemed significant if the statistics from both analysis methods indicated biases that were statistically different from zero. If only one analysis type exposed a bias statistically different from zero the bias was considered marginally significant.

A significant bias was revealed only for RS92-iMet temperature differences ($0.5 \pm 0.2\,^{\circ}$C). A marginally significant bias (−0.4 % RH) was exposed for the differences between frost point hygrometer-based RH values calculated using RS92 temperature and using iMet temperature. A second marginally significant bias (−1.2 % RH) was found for the differences between direct RH measurements by RS92 sondes and RH values calculated from frost point hygrometer measurements using iMet temperatures.

Altitude-dependent biases were assessed by dividing the 1-km median differences into 5-km altitude bins and performing the same statistical analyses on the differences in each bin. The overall RS92-iMet temperature bias ($0.5 \pm 0.2\,^{\circ}$C) was found to be independent of altitude. Even though no statistically significant bias was found for all RS92-iMet pressure differences, the 5-km bin analysis revealed an altitude-dependent progression of RS92-iMet pressure biases ranging from −0.6 hPa (0–5 km) to 0.7 ± 0.1 hPa above 15 km. Though some 5-km altitude-bin biases for RH differences are statistically or marginally significant, there is no indication of that RH measurement differences between any of the sensors have a statistically significant dependence on altitude.

We examined the quantitative impacts of pressure measurement differences between the RS92 and iMet sondes on water vapor mixing ratios calculated from frost point hygrometer measurements (FP_{RS92}-FP_{IMET}). No overall bias was revealed, but the altitude-dependent statistics of mixing ratio differences exposed statistically

AMTD
4, 4357–4401, 2011

significant biases of −2 % and −4 % in the 20–25 and 25–30 km bins, respectively. This evaluation illustrates how the accuracy of frost point hygrometer-based stratospheric water vapor mixing ratios very much depends on the accuracy of the requisite coincident pressure measurements.

Lastly we compared the altitudes calculated by each sounding system from incremental changes in pressure, temperature and RH measured by its own radiosonde. Altitude discrepancies between the RS92 and iMet systems are less than 0.1 km below 20 km, then increase with altitude to 0.2 km (20–25 km) and 0.4 km (25–30 km).

Acknowledgements. Thanks go to the entire staff of the JPL Table Mountain Facility for hosting and supporting the MOHAVE 2009 campaign at their magnificent facility. We are grateful for the assistance of Tony Grigsby, Monique Calhoun, and Dirisu Afusat during the campaign. NOAA provided the financial support for D. Hurst, E. Hall, and A. Jordan to participate in this campaign and funded the 4 NOAA FPHs that were flown.

References

Brewer, A. W., Cwilong, B., and Dobson, G. M. B.: Measurements of absolute humidity in extremely dry air, Proc. Phys. Soc., 60, 52–70, 1948.

Goff, J. A.: Saturation pressure of water on the new Kelvin temperature scale, Trans. Am. Soc. Heat. Ventilat. Eng., 63, 347–354, 1957.

Hurst, D. F., Oltmans, S. J., Vömel, H., Rosenlof, K. H., Davis, S. M., Ray, E. A., Hall, E. G., and Jordan, A. F.: Stratospheric water vapor trends over Boulder, Colorado: Analysis of the 30 year Boulder record, J. Geophys. Res., 116, D02306, doi:10.1029/2010JD015065, 2011.

Immler, F. J., Dykema, J., Gardiner, T., Whiteman, D. N., Thorne, P. W., and Vömel, H.: Reference Quality Upper-Air Measurements: guidance for developing GRUAN data products, Atmos. Meas. Tech., 3, 1217–1231, doi:10.5194/amt-3-1217-2010, 2010

Mastenbrook, H. J. and Oltmans, S. J.: Stratospheric water vapor variability for Washington, D.C./Boulder, CO; 1964-82, J. Atmos. Sci., 40, 2157–2165, 1983.

Miloshevich, L. M., Paukkunen, A., Vömel, H., and Oltmans, S. J.: Development and validation of a time-lag correction for Vaisala radiosonde humidity measurements, J. Atmos. Ocean. Tech., 21, 1305–1327, 2004.

AMTD
4, 4357–4401, 2011

Miloshevich, L. M., Vömel, H., Whiteman, D. N., and Leblanc, T.: Accuracy, assessment and correction of Vaisala RS92 radiosonde water vapor measurements, J. Geophys. Res., 114, D11305, doi:10.1029/2008JD011565, 2009.

Seidel, D. J., Angell, J. K., Christy, J., Free, M., Klein, S. A., Lanzante, J. R., Mears, C., Parker, D., Schabel, M., Spencer, R., Sterin, A., Thorne, P., and Wentz, F.: Uncertainty in signals of large-scale climate variations in radiosonde and satellite upper-air temperature datasets, J. Climate, 17, 2225–2240, doi:10.1175/1520-0442(2004)017<2225:UISOLC>2.0.CO;2, 2004.

Thorne, P. W., Parker, D. E., Christy, J. R., and Mears, C. A.: Uncertainties in climate trends: Lessons from upper-air temperature records, B. Am. Meteorol. Soc., 86, 1437–1442, doi:10.1175/BAMS-86-10-1437, 2005.

Titchner, H. A., Thorne, P. W., McCarthy, M. P., Tett, S. F. B., Haimberger, L., and Parker, D. E.: Critically reassessing tropospheric temperature trends from radiosondes using realistic validation experiments, J. Climate, 22, 465–485, doi:10.1175/2008JCLI2419.1, 2009.

Vömel, H., David, D. E., and Smith, K.: Accuracy of tropospheric and stratospheric water vapor measurements by the cryogenic frost point hygrometer: Instrumental details and observations, J. Geophys. Res., 112, D08305, doi:10.1029/2006JD007224, 2007a.

Vömel, H., Selkirk, H., Miloshevich, L., Valverde-Canossa, J., Valdes, J., Kyro, E., Kivi, R., Stolz, W., Peng, G., and Diaz, J. A.: Radiation dry bias of the Vaisala RS92 humidity sensor, J. Atmos. Ocean. Tech., 24, 953–963, doi:10.1175/JTECH2019.1, 2007b.

AMTD
4, 4357–4401, 2011

Table 1. Balloon Launches and Payloads.

Date, Time (UTC)	Flight	RS92	iMet	Frost Point
11 Oct, 08:23	TF022	2	1	CFH
15 Oct, 05:01	Oct15	2		
16 Oct, 04:19	TF024	1	1	FPH
16 Oct, 07:58	Oct16	2		
17 Oct, 04:47	TF025	2	1	CFH
17 Oct, 08:31	Oct17	2		
18 Oct, 02:55	TF026	1	1	FPH
18 Oct, 06:45	Oct18	2		
18 Oct, 21:11*	TF027	1	1	CFH
19 Oct, 03:31	TF028	2	1	CFH
19 Oct, 07:33	Oct19	2		
20 Oct, 05:11	TF029	1	1	CFH
20 Oct, 05:26	TF030	1	1	FPH
20 Oct, 08:11	TF031	1	1	CFH
20 Oct, 10:49	Oct20	2		
21 Oct, 06:08	TF033	2	1	CFH
21 Oct, 09:25	TF034	1	1	CFH
22 Oct, 02:58	TF035	1	1	CFH
22 Oct, 03:17	TF036	1	1	FPH
22 Oct, 10:34	TF037	1	1	CFH
22 Oct, 08:12	Oct22	2		
24 Oct, 03:21	TF038	1	1	CFH
24 Oct, 05:56	Oct24	2		
25 Oct, 03:55	TF039	2	1	CFH
25 Oct, 20:30*	TF040	1	1	CFH
26 Oct, 05:59	TF041	2	1	CFH
27 Oct, 05:17	TF042	1	1	CFH
27 Oct, 08:35	TF043	1	1	CFH

* Local daytime flights.

AMTD
4, 4357–4401, 2011

Table 2. Measurement Difference Statistics.

Parameter	Sensor 1[a]	Sensor 2	N[b]	Mean	Median	1 σ range		Inner-68 % Range		Units[c]
Temperature	RS92	iMet	26	0.54	0.48	−0.04	1.12	0.20	0.90	°C
Temperature	RS92	iMet	18	0.50	0.49	0.26	0.74	0.29	0.70	°C
Temperature	RS92	RS92b	14	−0.15	−0.02	−0.63	0.33	−0.43	0.13	°C
Temperature	RS92	RS92b	9	0.04	0.05	−0.06	0.14	−0.04	0.13	°C
Pressure	RS92	iMet	26	−0.01	0.39	−2.73	2.71	−0.63	1.00	hPa
Pressure	RS92	iMet	21	0.35	0.43	−0.33	1.03	−0.29	1.00	hPa
Pressure	RS92	RS92b	14	−0.14	−0.14	−0.37	0.09	−0.35	0.04	hPa
RH	RS92	RS92b	14	−0.4	−0.3	−1.4	0.5	−0.8	0.2	% RH
RH	RS92	RS92b	11	−0.3	−0.3	−0.7	0.1	−0.7	0.1	% RH
RH	FP_{RS92}	FP_{IMET}	26*	−0.9	−0.5	−2.1	0.4	−1.5	−0.1	% RH
RH	FP_{RS92}	FP_{IMET}	19*	−0.6	−0.4	−1.3	0.1	−1.0	−0.1	% RH
RH	RS92	FP_{RS92}	26*	−1.2	−0.9	−4.2	1.8	−2.4	0.3	% RH
RH	RS92	FP_{RS92}	21*	−0.8	−0.8	−2.2	0.6	−1.9	0.1	% RH
RH	RS92	FP_{IMET}	26*	−2.1	−1.4	−5.4	1.2	−3.5	−0.2	% RH
RH	RS92	FP_{IMET}	22*	−1.4	−1.2	−3.1	0.3	−2.8	−0.2	% RH
H_2O	FP_{RS92}	FP_{IMET}	26	−0.5	0.0	−2.2	1.1	−1.7	0.2	%
Altitude	RS92	iMet	26	−0.04	0.00	−0.15	0.07	−0.13	0.04	km
Altitude	RS92	RS92b	14	0.00	0.00	−0.04	0.04	−0.01	0.02	km

Statistics were computed from median differences in 1-km altitude bins for the number of profiles listed.

[a] Sensors FP_{RS92} and FP_{IMET} indicate the parameter was calculated from frost point hygrometer humidity measurements using coincident data from the RS92 and iMet radiosondes, respectively. RH calculations require temperature data while H_2O mixing ratio calculations require pressure data.

[b] The number of difference profiles considered. Rows with repeated parameters and sensors but a reduced number of profiles indicate that anomalous difference profiles were excluded. Asterisks for the number of RH difference profiles mean that only differences < 20 km were considered.

[c] Units for H_2O mixing ratios are percentage because the differences are relative to the mixing ratio.

AMTD
4, 4357–4401, 2011

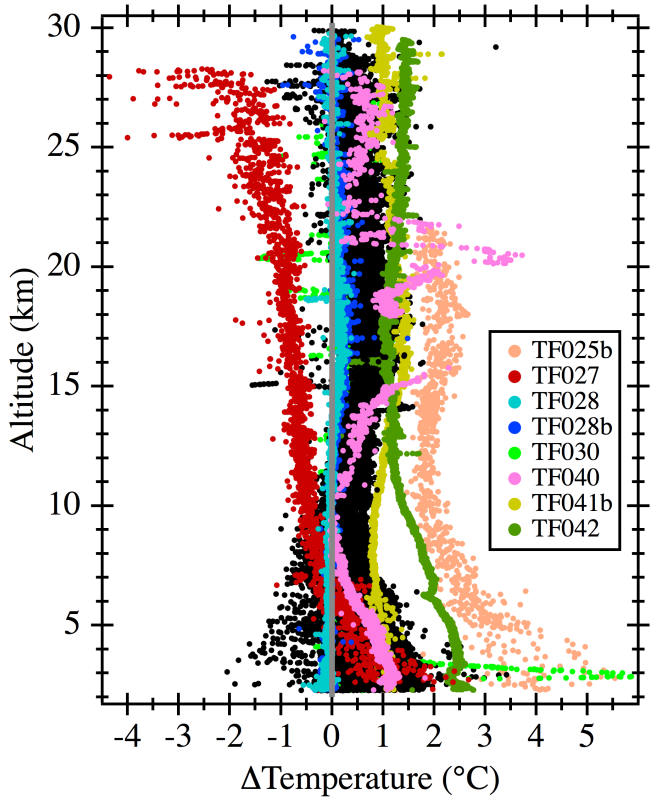

Fig. 1. All 26 profiles of temperature differences between RS92 and iMet radiosondes. Eight profiles are color-coded and identified as anomalous (non-conforming to the majority of difference profiles). Difference profiles designated by flight number and the suffix "*b*" are comparisons between secondary RS92 sondes and iMet sondes. The gray vertical zero line is included as a visual guide. Some random and large differences are caused by spurious measurement noise but the vast majority of differences present themselves as biases.

AMTD
4, 4357–4401, 2011

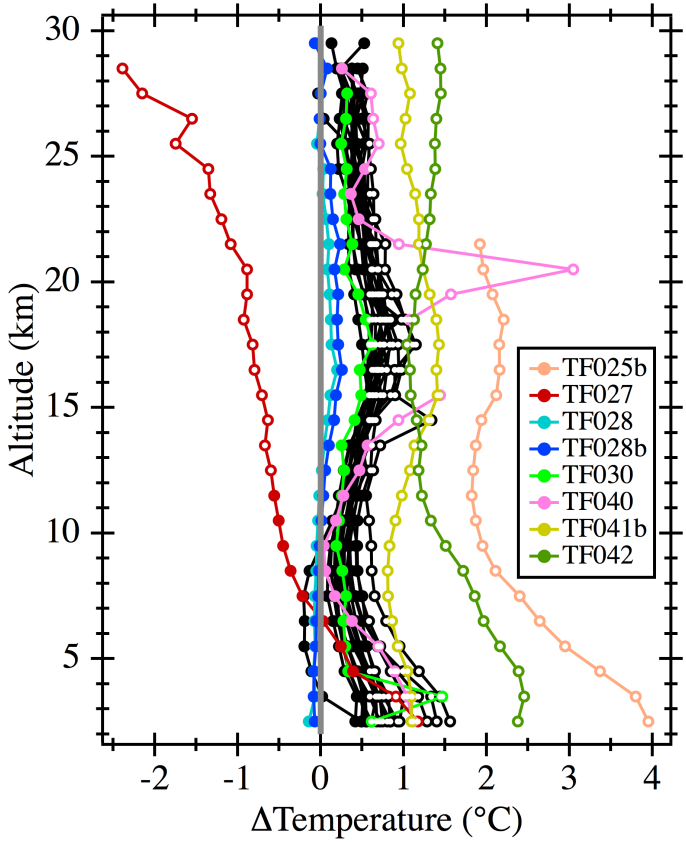

Fig. 2. Same as Fig. 1 except the RS92-iMet temperature differences are shown as median differences within 1-km altitude bins. Open circles depict median differences that exceed the combined manufacturer-quoted temperature measurement uncertainties (±0.58 °C). Two-thirds of these excessive temperature differences are concentrated between 14 and 22 km altitude.

AMTD
4, 4357–4401, 2011

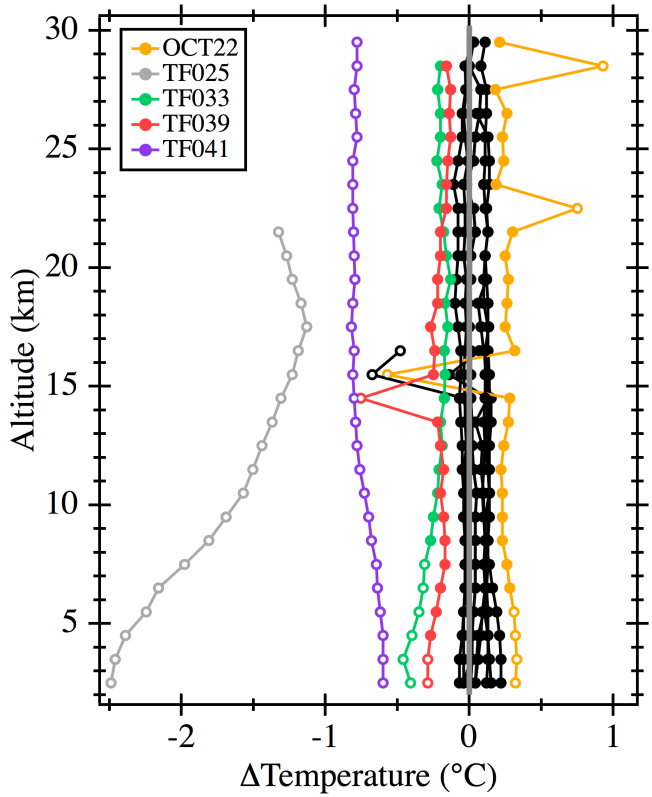

Fig. 3. All 14 profiles of median temperature differences between redundant RS92 sondes on the same balloons. Five anomalous difference profiles are identified by the flight number. Open circles depict 1-km median differences that exceed the combined manufacturer-quoted values for temperature measurement reproducibility (±0.28 °C below 16 km, ±0.42 °C above 16 km), representing 20 % of all median RS92-RS92 temperature differences. All but two of these excessive differences belong to the five anomalous profiles.

AMTD
4, 4357–4401, 2011

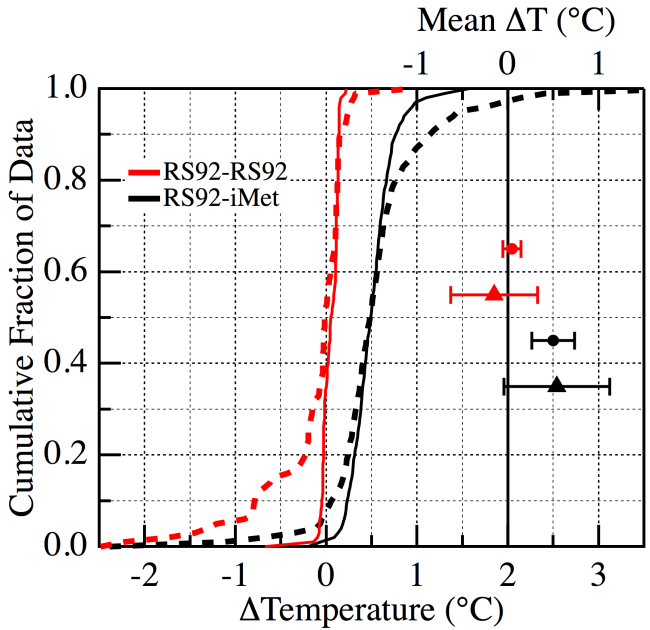

Fig. 4. Cumulative distribution functions and Gaussian statistics for RS92-RS92 (red curves) and RS92-iMet (black curves) temperature differences. The CDF data fractions (left axis) are associated with the bottom axis of temperature differences. Dashed and solid curves portray the CDFs for the differences in all profiles and the differences in the majority of profiles, respectively. The dashed black curve extends off the graph to a maximum temperature difference of 3.9 °C. Mean values and their standard deviations (horizontal bars) for all the differences (triangles) and for the majority of differences (dots) are shown to the right of the CDFs. These mean values for RS92-RS92 (red) and RS92-iMet (black) differences are associated with the top axis scale and the vertical black zero line. The mean and standard deviation range for RS92-iMet differences (black dot) reveals a statistically significant positive bias of about 0.5 ± 0.2 °C.

AMTD
4, 4357–4401, 2011

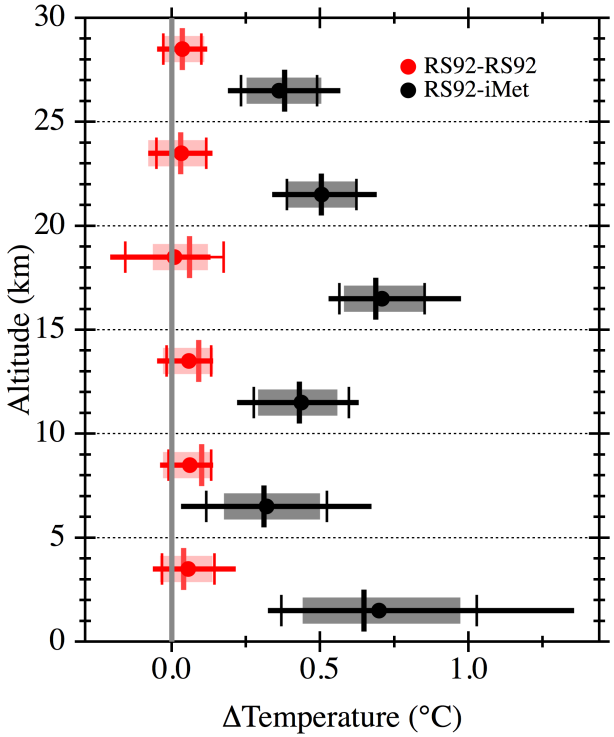

Fig. 5. Altitude-dependent statistics of RS92-iMet (black) and RS92-RS92 (red) temperature differences in 5-km altitude bins. The mean (dot), median (thick vertical dash), inner-68 % range (shaded box), standard deviation range (bounded by two thin vertical dashes) and inner-90 % range (5th to 95 th percentile, horizontal lines) of the 1-km median temperature differences in the majority of profiles are presented. Agreement between mean and median values, and between the inner-68 % and standard deviation ranges visually indicates the distribution of differences in the bin is near normal. If these ranges do not cross the vertical zero line the mean and median biases are statistically significant, as is the case for the RS92-iMet temperature bias in every 5-km bin.

AMTD
4, 4357–4401, 2011

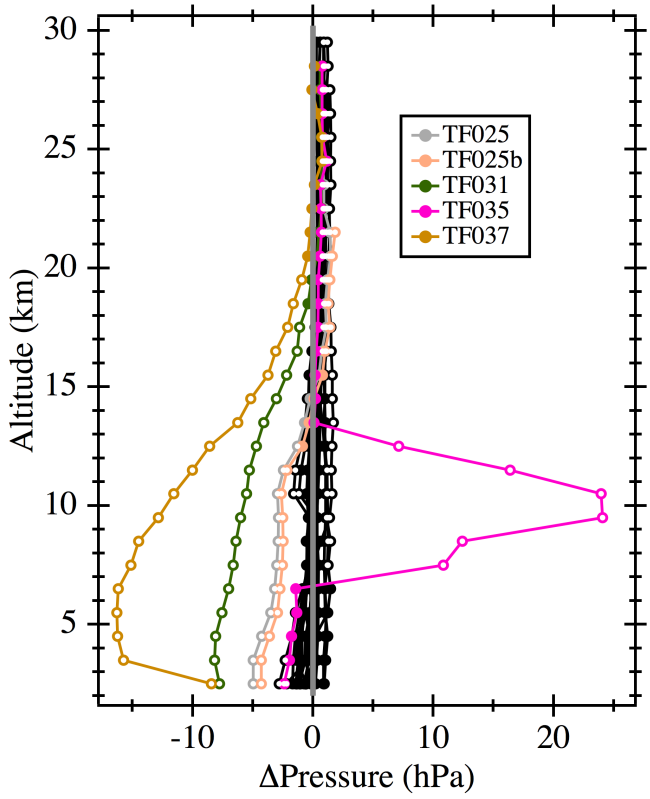

Fig. 6. All 26 profiles of median 1-km altitude-binned pressure differences between RS92 and iMet radiosondes, of which 5 are identified as anomalous. About 30 % of these pressure differences (open circles) exceed the combined manufacturer-quoted uncertainty limits. Eighty-three percent of these excessive differences are above 16 km altitude where the quoted measurement uncertainty limits are smallest.

AMTD
4, 4357–4401, 2011

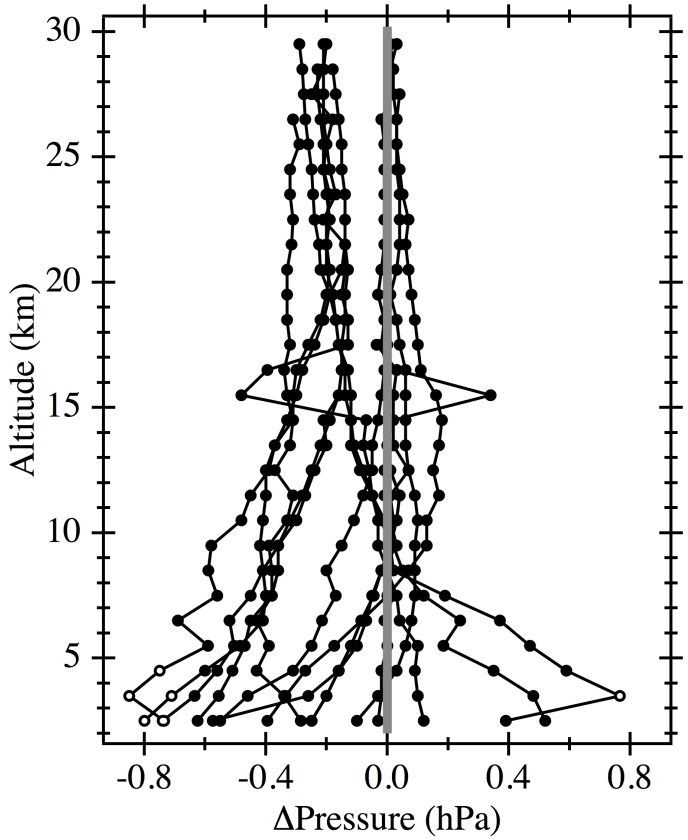

Fig. 7. Fourteen profiles of median pressure differences between redundant RS92 sondes on the same balloons. None of the difference profiles are identified as anomalous. Only 7 (2 %) of the pressure differences exceed the manufacturer-quoted limits for RS92 pressure measurement reproducibility.

AMTD
4, 4357–4401, 2011

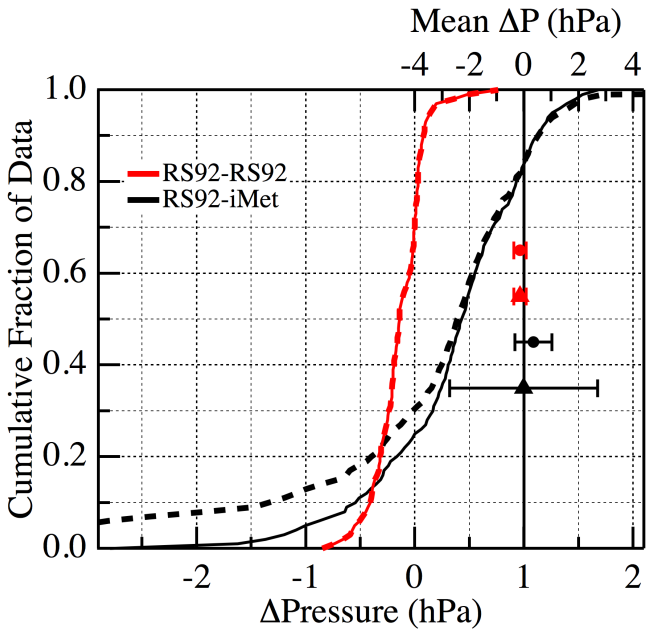

Fig. 8. CDFs and Gaussian statistics for RS92-RS92 and RS92-iMet pressure differences, as in Fig. 4 for temperature differences. The red dashed and solid curves are identical because none of the RS92-RS92 difference profiles were anomalous. The black dashed curve extends off the graph to minimum and maximum values of −16.3 and 24.1 hPa. Though the CDFs of RS92-iMet differences are positively shifted by about 0.5 hPa, the mean values and their standard deviation ranges reveal no significant biases in the pressure differences.

AMTD
4, 4357–4401, 2011

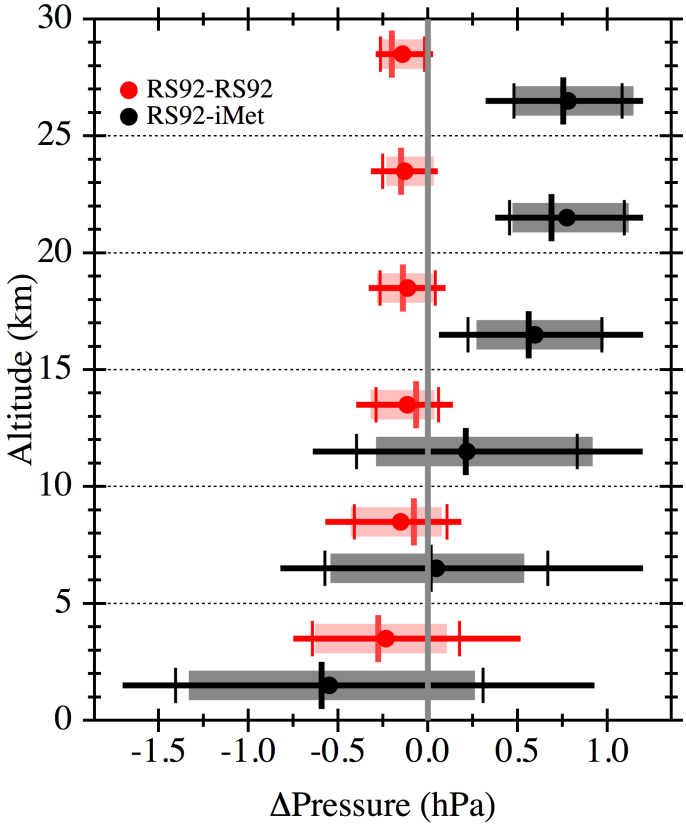

Fig. 9. Five-km altitude-bin statistics for for RS92-iMet (black) and RS92-RS92 (red) pressure differences. Statistics for the RS92-iMet pressure differences reveal statistically significant positive biases above 15 km.

AMTD
4, 4357–4401, 2011

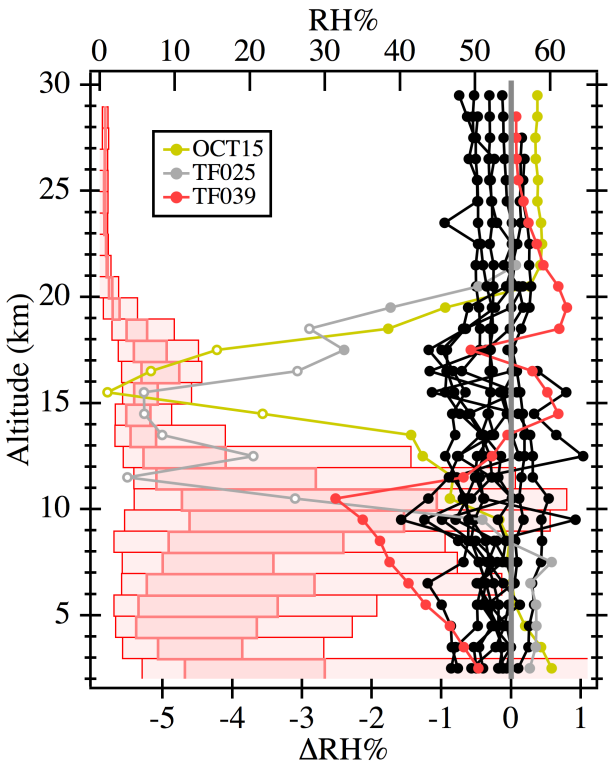

Fig. 10. Fourteen profiles of 1-km median RH differences between redundant RS92 sondes, of which 3 are anomalous. Only 4 % of the differences exceed the manufacturer-quoted limits of measurement reproducibility. The light and dark red horizontal bars depict the inner-90 % ranges and interquartile ranges, respectively, of RS92 RH measurements within 1-km altitude bins, relative to the top axis scale. These illustrate how RH values become small at about 20 km, above which only 5 % of RH values are >3 % RH. This dramatic decline in RH values limits the % RH differences above 20 km to small values.

AMTD
4, 4357–4401, 2011

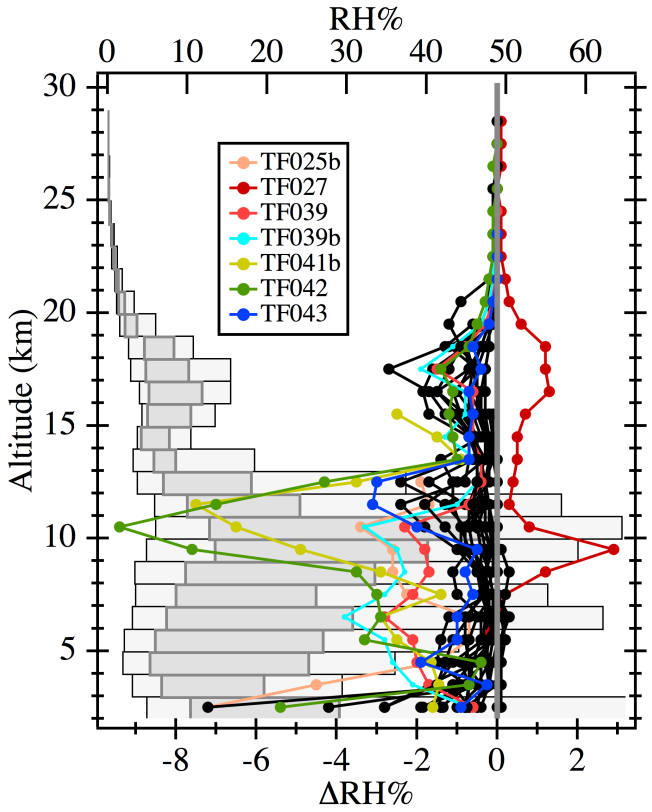

Fig. 11. Twenty-six profiles of median differences between RH values calculated from frost point hygrometer measurements using RS92 temperatures (FP_{RS92}) and iMet temperatures (FP_{IMET}). Four of the 7 anomalous RH difference profiles here were also identified as anomalous for RS92-iMet temperature differences (Fig. 2). The inner-90 % and interquartile ranges of FP_{RS92} RH values, as in Fig. 10 but here depicted by light and dark gray horizontal bars, respectively, show the same altitude dependence of RH values above 20 km.

AMTD
4, 4357–4401, 2011

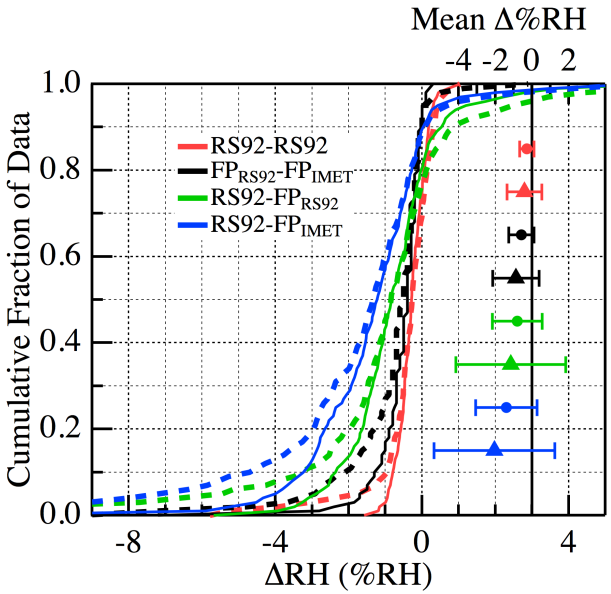

Fig. 12. The CDFs and Gaussian statistics for RS92-RS92, FP_{RS92}-FP_{IMET}, RS92-FP_{RS92} and RS92-FP_{IMET} relative humidity differences. The latter two sets of differences are between RS92 direct RH measurements and RH values calculated from frost point hygrometer measurements using RS92 and iMet temperatures, respectively. The RH difference values above 20 km were excluded from every comparison except RS92-RS92 (see text). The RS92-FP_{RS92} and RS92-FP_{IMET} CDFs for all difference profiles (green dashed and blue dashed curves, respectively) extend off the graph to minimum values of −22.1 and −24.1 % RH, respectively. Though the CDFs for each set of RH differences presented here are shifted to the left of zero, none of the means and standard deviation ranges of the RH differences expose a significant bias.

AMTD
4, 4357–4401, 2011

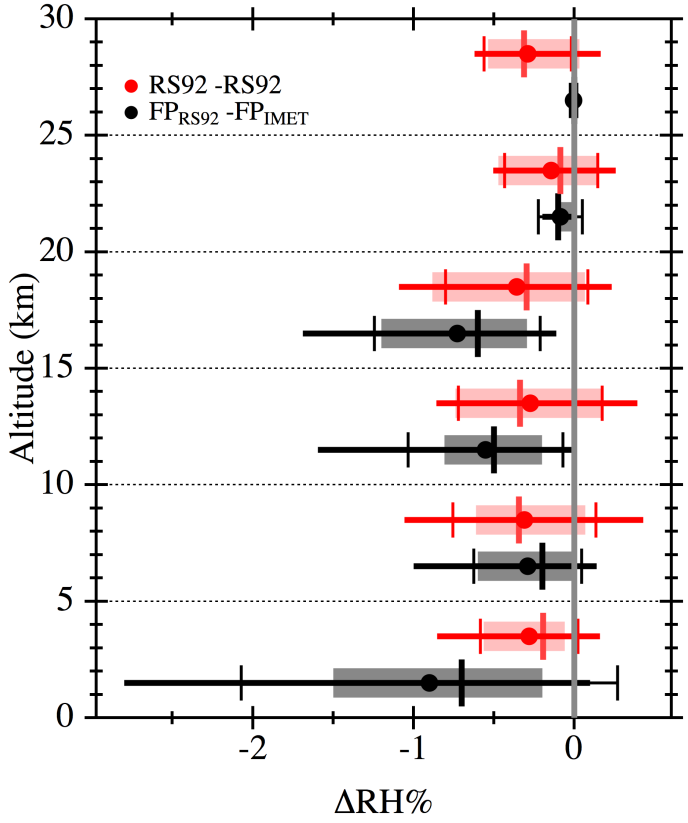

Fig. 13. Five-km altitude-bin statistics for RS92-RS92 (red) and FP_{RS92}-FP_{IMET} (black) RH differences. Only the negative FP_{RS92}-FP_{IMET} (black) RH differences in the 10–15 and 15–20 km bins reveal significant biases.

AMTD
4, 4357–4401, 2011

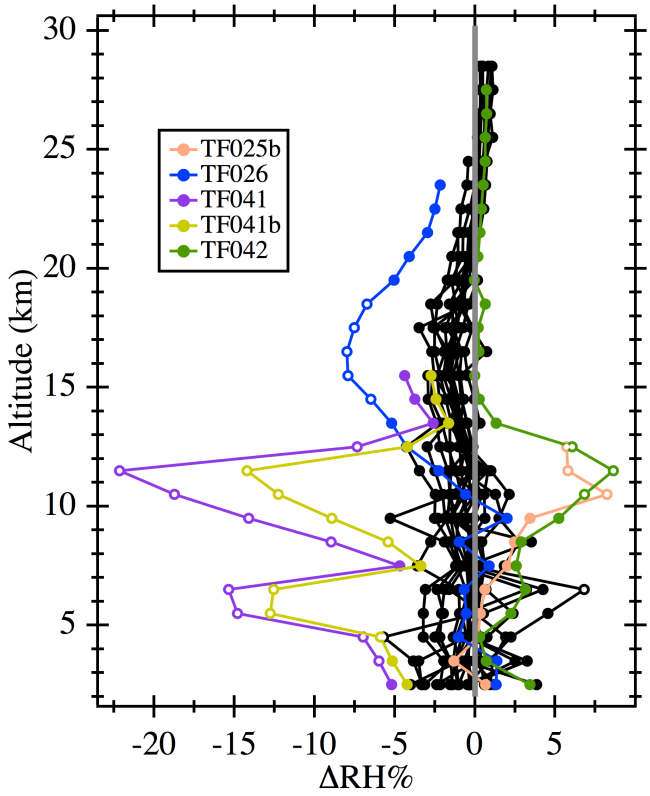

Fig. 14. All 26 profiles of median differences between RH measured directly by RS92 sondes and RH values calculated from frost point hygrometer measurements using coincident RS92 temperature data (RS92-FP_{RS92}). Five profiles are identified as anomalous. Ninety-one percent of the RH differences are within the manufacturer-quoted measurement uncertainty limits of ±5 % RH.

AMTD
4, 4357–4401, 2011

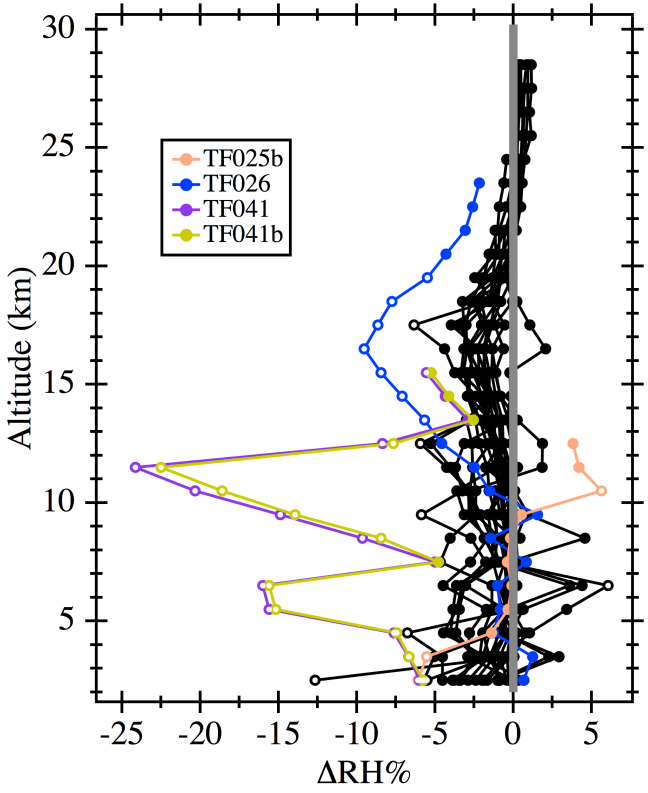

Fig. 15. Twenty-six profiles of median differences between RH measured directly by RS92 sondes and RH values calculated from frost point hygrometer measurements using coincident iMet temperature data (RS92-FP_{IMET}). Four profiles identified as anomalous in Fig. 14 are also identified here. Ninety percent of the RH differences are within the manufacturer-quoted measurement uncertainty limits of ±5 % RH.

AMTD
4, 4357–4401, 2011

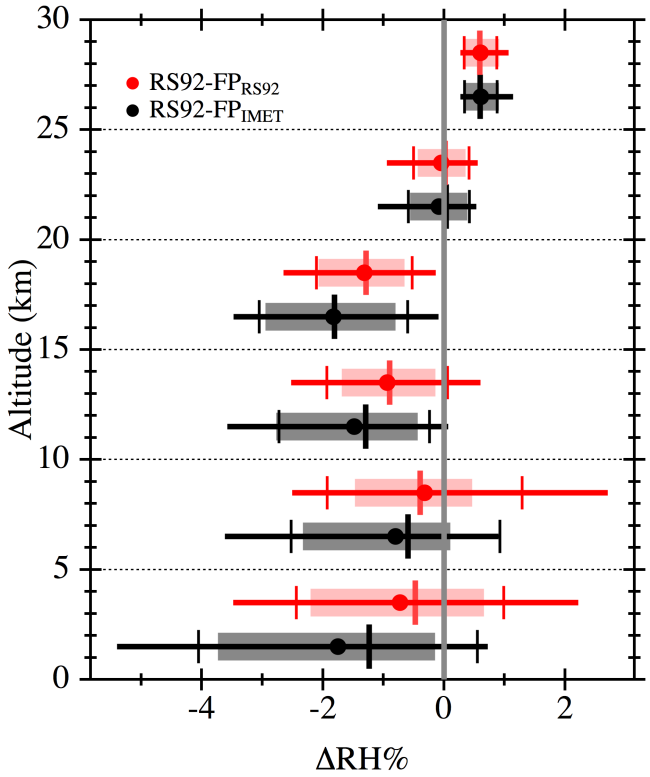

Fig. 16. Five-km altitude-bin statistics for RS92-FP$_{RS92}$ (red) and RS92-FP$_{IMET}$ (black) RH differences. There are significant negative biases in RS92-FP$_{IMET}$ differences (10–15 and 15–20 km) and RS92-FP$_{RS92}$ differences (15–20 km), and significant positive biases in both sets of RH differences in the 25–30 km bin.

AMTD
4, 4357–4401, 2011

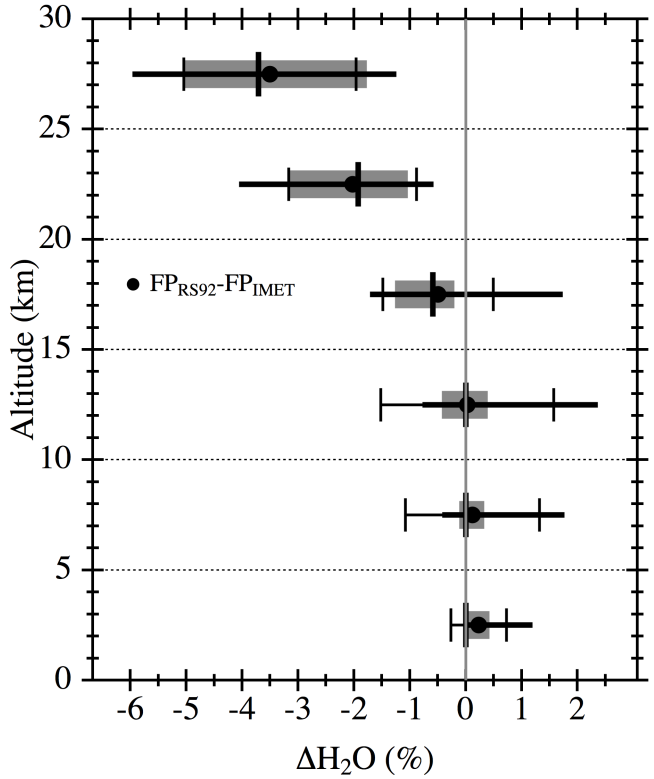

Fig. 17. Five-km altitude-bin statistics for relative differences in water vapor mixing ratios calculated from frost point hygrometer measurements using RS92 pressure (FP_{RS92}) and iMet pressure (FP_{IMET}). Statistics for the differences above 20 km reveal significant negative biases at the highest altitudes.

AMTD
4, 4357–4401, 2011

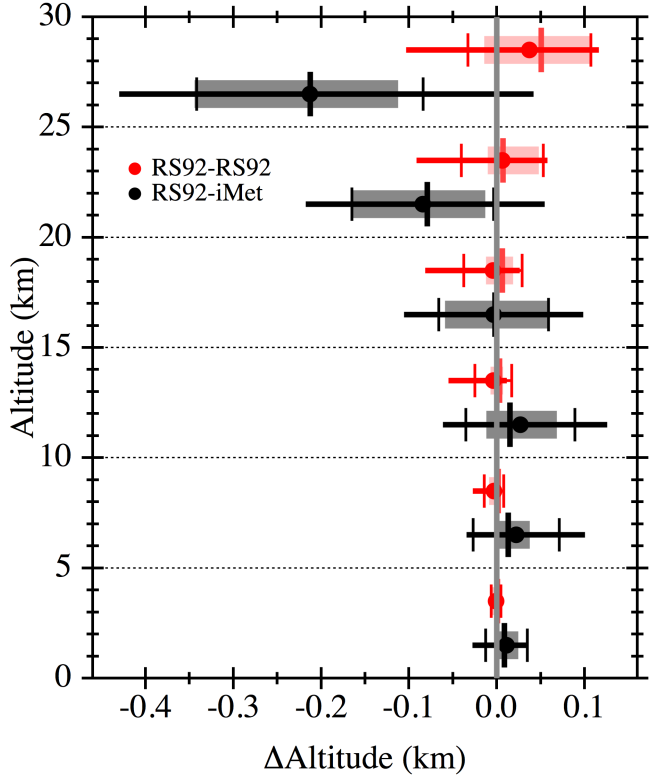

Fig. 18. Five-km altitude-bin statistics for altitude differences between redundant RS92 sondes (red) and between RS92 and iMet sondes (black). Only the large negative RS92-iMet differences above 25 km depict a significant bias.

AMTD
4, 4357–4401, 2011